

Master Equation Analysis of Thermal Activation Reactions: Reversible Isomerization and Decomposition

Vladimir M. Bedanov,[†] Wing Tsang,* and Michael R. Zachariah

Chemical Science and Technology Laboratory, National Institute of Standards and Technology, Gaithersburg, Maryland 20899

Received: April 3, 1995; In Final Form: May 11, 1995[§]

We present the full solution of the master equation for the system with reversible isomerization and decomposition channels at low pressures. As an example of such a system we consider the *cis-trans* isomerization of 2-butene. At high temperatures *cis*-2-butene decomposes into butadiene and hydrogen. The effect of isomerization on the decomposition rate coefficient was studied and indicated multiple steady-state behavior. At 1200 K, for example, a true steady state is achieved only after 75% of the product has been formed. This behavior is explained in terms of relaxation to the equilibrium distribution between *cis* and *trans* isomers. The first plateau in the rate coefficient corresponds to the irreversible regime of isomerization when two isomers are far from equilibrium, while the second plateau or true steady state is established after equilibrium between isomers has been reached. The effect is not observed at either low temperatures or high pressures.

I. Introduction

Many chemical processes, particularly those involving large polyatomic compounds, include both reversible isomerizations and decompositions. Some of these are of great practical importance, for example, the decomposition and isomerization pathways of large organic radicals in combustion environments. In this paper we treat a particularly simple case,



where A is a reactant, which can either isomerize reversibly to B or decompose to a product C (Figure 1). At present, only studies on separate parts of the reaction are known from the literature: the irreversible reaction A → C is well described by the theory of unimolecular reactions^{1–3} and reversible isomerization reactions A ⇌ B have been studied recently by the master equation analysis.^{4–6} However, the full scheme has not been investigated in a self-consistent manner. It is unclear how strong the effect of isomerization is and under what conditions we can neglect the isomerization and apply a simple irreversible scheme for the formation rate of C.

The purpose of this work is to present a detailed study on the basis of solution to the time-dependent master equation for the system involving isomerization and decomposition. As a reference system we consider *cis-trans* isomerization of 2-butene. This system has been well investigated experimentally.^{7–10} The rate coefficient for the isomerization was measured over a wide range of pressures and temperatures. It was found^{8,10} that at temperatures higher than 1250 K, formation of butadiene starts to interfere with the isomerization. When interpreting the high-temperature and low-pressure experimental data, it was suggested¹⁰ that isomerization is much faster than decomposition, such that *cis*- and *trans*-2-butene are in equilibrium. Here, we will present master equation analysis for the system under the same conditions to examine this assumption.

In section II, we describe the master equation and the computational method we used to solve the eigenvalue problem

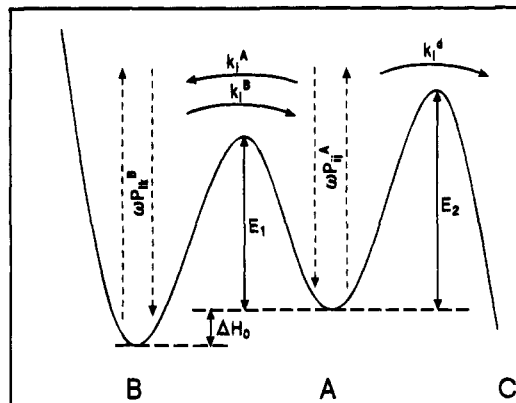


Figure 1. Schematic energy diagram for a system with isomerization and decomposition channels described by eqs 1.

for the relaxation matrix. In section III, results of calculations for the isomerization of *cis*-2-butene at low temperatures are presented and compared with the Rabinovitch and Michel⁸ measurements. High-temperature calculations are discussed in section IV, where we give a new interpretation of the experiment¹⁰ on very low-pressure pyrolysis of *cis*-2-butene.

II. The Master Equation

The time evolution of the system may be described by a master equation.³ In the discrete formulation, the master equation for the system with reversible isomerization and decomposition may be written as

$$\frac{d\varrho_i^A}{dt} = \omega \sum_j P_{ij}^A \varrho_j^A - \omega \varrho_i^A - k_i^A \varrho_i^A - k_i^d \varrho_i^A + k_i^B \varrho_i^B \quad (1a)$$

$$\frac{d\varrho_i^B}{dt} = \omega \sum_k P_{ik}^B \varrho_k^B - \omega \varrho_i^B - k_i^B \varrho_i^B + k_i^A \varrho_i^A \quad (1b)$$

where ϱ_i is the population of the i th energy level, k_i is the microscopic (energy dependent) rate coefficient, P_{ij} are collision energy transfer probabilities, and ω is the collision frequency.

[†] Permanent address: Institute of Theoretical and Applied Mechanics, Novosibirsk, 630090, Russia.

[§] Abstract published in *Advance ACS Abstracts*, June 15, 1995.

Superscripts A, B, and d denote the two isomers and the decomposition channel, respectively. Index l for isomer B corresponds to the same energy as i for A, $E_i = E_l$. The first term on the right side of each of the equations stands for gain by collisional energy transfer from all other levels E_j (in eq 1a) with rate coefficient ωP_{ij} . The second stands for loss by collisional energy transfer to all other levels and we used in this expression the normalization condition for collision energy transfer probabilities

$$\sum_j P_{ij} = 1 \quad (2)$$

Other terms are loss and gain by different reaction channels with corresponding rate coefficients.

In real calculations, infinite sums over energy levels in eqs 1 are replaced by finite sums with a cutoff energy high enough to ensure the population of the highest levels to be negligibly small. Taking the cutoff energy as large as $2E_0$, where E_0 is the threshold energy, provided sufficient computational accuracy. The energy grain size was chosen such that there were ~ 150 grains for each isomer.

The collision energy transfer probabilities were taken in the standard form of an "exponential down" model

$$P_{ij} = A_j \exp(-(E_j - E_i)/\alpha), \quad j \geq i \quad (3)$$

where α is a positive parameter governing the magnitude of the energy transfer, with corresponding upward probabilities obtained from detailed balance

$$P_{ji}f_i = P_{ij}f_j \quad (4)$$

where f_i is the equilibrium distribution function

$$f_i = \frac{1}{Q} N_i \exp\left(-\frac{E_i}{k_B T}\right) \quad (5)$$

where k_B is the Boltzmann constant, Q is the partition function, and N_i is the density of states. Normalization constants A_j are found from the normalization condition eq 2 by using a recursive algorithm described by Gilbert and Smith.³

The microscopic rate coefficients $k(E)$ were calculated by using RRKM theory, which leads to

$$k(E) = l^{\ddagger} \frac{G^{\ddagger}(E)}{hN(E + E_0)} \quad (6)$$

where $G^{\ddagger}(E)$ is the total number of states of the transition structure, up to and including E , $N(E)$ is the density of states of the reactant, and l^{\ddagger} is the reaction path degeneracy. $G^{\ddagger}(E)$ and $N(E)$ were calculated from the set of vibrational frequencies using the fast algorithm for direct count of Beyer and Swinehart.^{3,11}

The coefficient for the reverse reaction is obtained by detailed balance

$$k_i^A N_i^A = k_l^B N_l^B \quad (7)$$

It is convenient to consider the master equation (eq 1) in matrix form. We introduce a vector ρ , whose first M elements are ρ_i^A and elements from $M + 1$ to $2M - h$ are ρ_l^B , $h = \Delta H/\delta E$ accounts for a difference in zero-point levels for two isomers. Then we can rewrite eq 1 in the form

$$d\rho/dt = \mathbf{J}\rho \quad (8)$$

where \mathbf{J} is the relaxation matrix constructed from the energy transfer probabilities and the microscopic rate coefficients. The formal solution of eq 8 is

$$\rho(t) = e^{Jt}\rho(0) \quad (9)$$

where $\rho(0)$ is the initial population vector. The solution can be expressed in terms of eigenvectors and eigenvalues of \mathbf{J} . However, because most methods of diagonalization are developed for symmetric (Hermitian) matrices,¹² it is useful first to transform \mathbf{J} to a symmetric matrix

$$\mathbf{B} = \mathbf{F}\mathbf{J}\mathbf{F}^{-1} \quad (10)$$

where \mathbf{F} is a diagonal matrix with the elements³

$$F_{ii} = \frac{1}{f_i^{1/2}}, \quad i = 1, 2, \dots, 2M - h \quad (11)$$

Equation 9 now becomes

$$\rho(t) = \mathbf{F}^{-1} e^{Bt} \mathbf{F} \rho(0) \quad (12)$$

Matrix \mathbf{B} can be expressed in the form

$$\mathbf{B} = \mathbf{U}^{-1} \mathbf{A} \mathbf{U} \quad (13)$$

where \mathbf{A} is the diagonalized form of eigenvalues, \mathbf{U} is a matrix, which consists of the components of the eigenvectors of \mathbf{B}

$$U_{ij} = (S_i)_j \quad (14a)$$

$$(U^{-1})_{ij} = (S_j)_i \quad (14b)$$

where $(S_i)_j$ stands for the j th component of the i th eigenvector.

Now we can rewrite eq 9 as

$$\rho(t) = \mathbf{F}^{-1} \mathbf{U}^{-1} e^{\Lambda t} \mathbf{U} \mathbf{F} \rho(0) \quad (15)$$

and substituting expressions 11 and 14 for \mathbf{F} and \mathbf{U} we obtain

$$\rho_i(t) = \sum_j f_i^{1/2} (S_j)_i e^{\lambda_j t} \sum_k (S_j)_k \frac{1}{f_k^{1/2}} \rho_k(0) \quad (16)$$

Note that indexes i and j run here from 1 to $2M - h$.

In our computations we symmetrize \mathbf{J} as described above; then we apply Householder's algorithm¹² for tridiagonalization and after that the implicit QR algorithm¹² for final diagonalization. This procedure provides a fast and stable method to find a complete set of eigenvectors and eigenvalues of \mathbf{J} .

Once eigenvalues λ_i and eigenvectors S_i are found, one can calculate the population function ρ for each isomer as a function of time (eq 16) and the time-dependent forward and reverse reaction rate coefficients for the isomerization

$$k_f = \sum_i k_i^A \rho_i^A / \sum_i \rho_i^A \quad (17a)$$

$$k_r = \sum_l k_l^B \rho_l^B / \sum_l \rho_l^B \quad (17b)$$

and decomposition rate coefficient

$$k_d = \sum_i k_i^d \rho_i^A / \sum_i \rho_i^A \quad (18)$$

It should be noted that rate coefficient k_d is directly measured in experiments, while k_f and k_r are usually calculated through

other measured parameters. For example, in the case of equilibrating isomerization without exit channel, $k_f^{(e)}$ and $k_r^{(e)}$ are calculated through relaxation coefficient k_{rel} and equilibrium constant K_c^{eq}

$$k_f^{(e)} = k_{\text{rel}} \left(\frac{K_c^{\text{eq}}}{1 + K_c^{\text{eq}}} \right) \quad (19a)$$

$$k_r^{(e)} = k_{\text{rel}} \left(\frac{1}{1 + K_c^{\text{eq}}} \right) \quad (19b)$$

where k_{rel} is the rate coefficient describing the approach to equilibrium (but not the rate of isomerization!), which is defined through the slope of time dependence of the displacement from the equilibrium concentration of one of the isomers. The relationship between k_f and k_r extracted from the experimental data and those defined by eqs 17 has been discussed in the literature^{4–6} and shown not to be equivalent. Therefore, in order to compare our calculations with experimental data on equilibrating isomerization we need to compute k_{rel} . Following Quack⁴ we define a phenomenological relaxation coefficient k_{rel} as

$$k_{\text{rel}}(t) = - \frac{1}{\Delta A(t)} \frac{d}{dt} \Delta A(t) \quad (20)$$

where $\Delta A(t) = A(t) - A(\infty)$ is the displacement from the equilibrium concentration for isomer A. In practical calculations k_{rel} may be determined via the equation⁵

$$k_{\text{rel}}(t) = \frac{\sum k_i^A \varrho_i^A(t) - \sum k_i^B \varrho_i^B(t)}{A(t) - A(\infty)} \quad (21)$$

At very low pressures, the collision frequency between gas molecules becomes comparable to the wall collision frequencies, such that wall collisions contribute to the energy transfer rate. The easiest way to account for a wall effect is to make a correction to the collision frequency ω . The molecule–molecule collision frequency is

$$\omega_g = [M] \left[\frac{8k_B T}{\pi \mu} \right]^{1/2} \pi d^2 \quad (22)$$

where $[M]$ is the concentration of bath gas, μ is the reduced mass, and d is the collision diameter. The wall collision frequency is

$$\omega_w = \left[\frac{8k_B T}{\pi m} \right]^{1/2} \frac{S}{V} \quad (23)$$

where m is the molecule mass and S and V are the surface and the volume of the vessel. We can replace the collision frequency in eqs 1 with $\omega = \omega_g + \omega_w$, which is a linear function of pressure and finite at $[M] = 0$. Since the collision energy transfer probabilities may be different for the two types of collisions, it is reasonable to define α in eq 3 to have the form

$$\alpha = \frac{\alpha_g \omega_g + \alpha_w \omega_w}{\omega_g + \omega_w} \quad (24)$$

where α_g and α_w correspond to molecule and wall collisions, respectively.

III. Equilibrating Isomerization (No Decomposition)

We consider *cis*-2-butene as an example of a real system to which we can apply our computational scheme. Isomerization

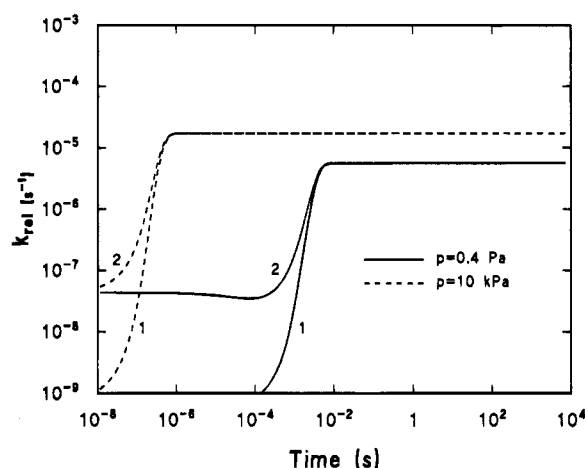


Figure 2. Relaxation rate coefficient as a function of time. Non-steady-state master equation analysis of equilibrating *cis*–*trans* isomerization of 2-butene at $T = 742$ K. Each calculation is made for two different initial distributions for *cis* isomer: $T_0 = 300$ (1) and 600 (2) K.

of *cis*-2-butene to *trans*-2-butene is well investigated experimentally.^{8–10} At temperatures below 1250 K it is practically a pure isomerization with a negligible amount of side products formation,^{8,9} while at higher temperatures, the relative importance of side products sharply increases.^{9–10} The main channel for side reactions is decomposition of *cis*-2-butene to butadiene and hydrogen.¹⁰

In this section we consider low-temperature isomerization of *cis*-2-butene at $T = 742.2$ K, where equilibrating isomerization was studied by Rabinovitch and Michel⁸ in a wide range of pressures. In our calculations we used the following parameters from refs 14 and 15: $\ell^* = 2$, $d = 5.0$ Å, $\Delta H_0 = -350$ cm⁻¹, $E_1 = 21\,900$ cm⁻¹, where ΔH_0 is the heat of reaction at 0 K and E_1 the activation energy for the forward reaction at 0 K (Figure 1). In our notation now A = *cis* and B = *trans*. The vibrational frequencies for *cis* and *trans*-2-butene were taken as reported by Richards and Nielsen.¹³ The vibrational frequencies for the activated complex were used as assigned by Lin and Laidler¹⁴ which were obtained by fitting to the high-pressure results of Rabinovitch and Michel⁸ and Lifshitz, Bauer, and Resler.⁹ Initial population was set to zero for *trans* isomer and an equilibrium distribution for vibrational–rotational states of the *cis* isomer corresponding to temperature T_0 .

Figure 2 shows the time evolution of the relaxation rate coefficient for *cis*–*trans* isomerization of 2-butene at $T = 742$ K at low and high pressures. Each calculation was done for two different initial populations corresponding to $T_0 = 300$ K and $T_0 = 600$ K. The results show that the final steady-state rate constant does not depend on initial population, and the induction time required to achieve a steady state decreases with increasing pressure.

A comparison of calculated steady-state rate coefficients with the experimental data of Rabinovitch and Michel⁸ is shown in Figure 3. The calculations were made for both the finite system (solid line) corresponding to the reactor size of 4250 cm³ (big bulb used by Rabinovitch and Michel⁸ at low pressures) and for the infinite system (dashed line) using the following parameters for collision energy transfer probabilities: $\alpha_g = 300$ cm⁻¹ and $\alpha_w = 800$ cm⁻¹. When calculating the correction for the wall collisions we assumed a cylindrical reactor with the length to diameter ratio of 2. Our results reproduce measured rate coefficients very well. Note that at low pressures, there is significant deviation from the standard falloff curve (dashed line) resulting from wall collisions, because, at these

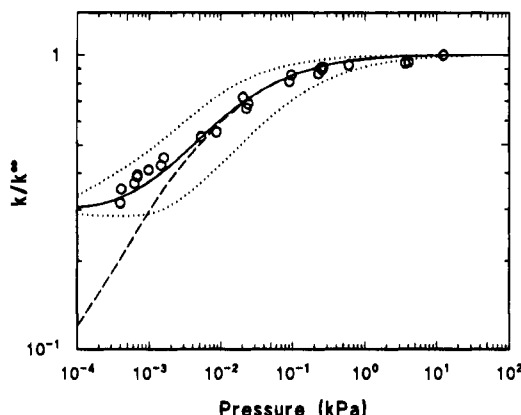


Figure 3. Falloff curves for *cis-trans* isomerization of 2-butene at $T = 742\text{ K}$: experiment of Rabinovitch and Michel⁸ (circles), master equation for the infinite system (dashed line), master equation for the 4250 cm^3 reactor used in the experiment⁸ (solid line). Dotted lines are same calculations but with $\alpha_g = 600$ (upper curves) and 150 cm^{-1} (lower curve).

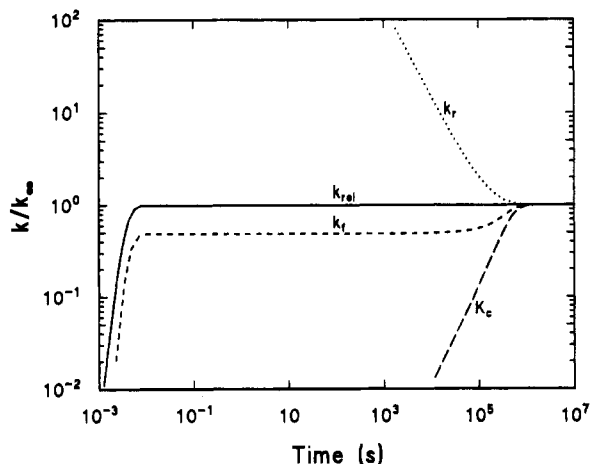


Figure 4. Time evolution of constant K_c and rate coefficients k_f , k_r , and k_{rel} . Equilibrium between A (*cis*) and B (*trans*) isomers is achieved at $\sim 10^6\text{ s}$, which corresponds to the second plateau for k_f . The first plateau of k_f corresponds to the irreversible regime of isomerization.

pressures, both of the collision frequencies are comparable: $w_g = 23\,000\text{ s}^{-1}$ and $w_w = 19\,000\text{ s}^{-1}$ at $p = 4 \times 10^{-4}\text{ kPa}$.

Figure 4 shows time dependencies of k_{rel} , k_f , k_r , and nonequilibrium $K_c = B/A$ up to 10^7 s at $T = 742\text{ K}$ and $p = 4 \times 10^{-4}\text{ kPa}$. At $t > 10^6\text{ s}$, the system has established equilibrium, as all quantities shown in Figure 4 have achieved their $t = \infty$ values. However, the process of equilibration itself is in steady state (k_{rel} is constant at $t > 10^2\text{ s}$). For comparison purposes the duration of a typical run in Rabinovitch-Michel experiment⁸ is hundreds of seconds, which corresponds to steady-state relaxation, more exactly, to the early stages of it, where the isomers are still far from equilibrium (Figure 4).

An interesting feature seen in Figure 4 is that the forward rate coefficient k_f is time independent in the interval $10^{-2}\text{ s} < t < 10^4\text{ s}$ and then grows gradually and reaches its true steady-state value k_f^∞ at $\sim 10^6\text{ s}$. During the initial stages of the steady-state equilibration process, the *trans* isomer is poorly populated, and the isomerization behaves essentially irreversibly, which can be expressed in terms of four-state model:



Note, however, this is not a purely irreversible process like in

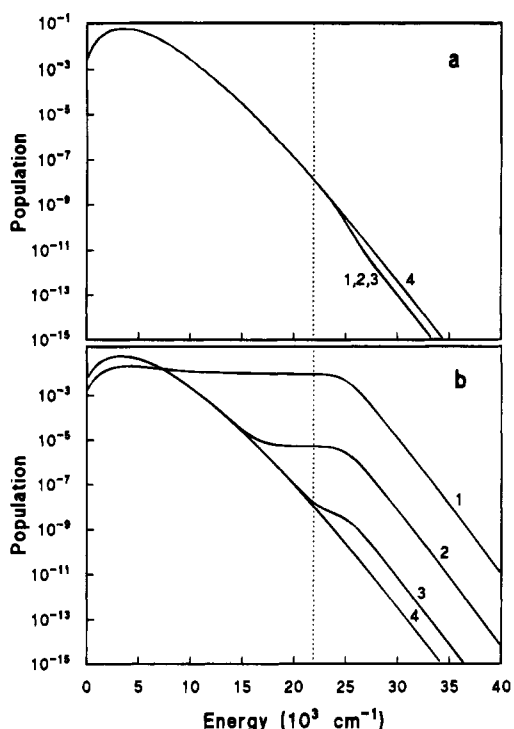


Figure 5. Normalized population of energy levels of isomer A (*cis*) (a) and B (*trans*) (b) during irreversible isomerization (1, 2, 3) and at very late stages of equilibrating process (4). Time in seconds: 10^2 (1), 10^3 (2), 10^4 (3), and 10^6 (4). Dotted line corresponds to the threshold for isomerization.

the case of unimolecular decomposition. In this three-step reaction, only one step, which is collisional deactivation of isomer B, is irreversible, while the other two, collisional activation and deactivation of isomer A and conversion between energized species, are reversible. This class of irreversible processes has been studied by Green et al.,⁵ who identified the phenomenological rate coefficients eqs 19a and 19b with the steady-state net flux of reaction in forward and reverse directions, respectively. In our case, the net flux of reaction is

$$k_{A \rightarrow B}^{\text{net}} = \frac{\sum \varrho_i^A k_i^A - \sum \varrho_i^B k_i^B}{\sum \varrho_i^A} \quad (25)$$

So, comparing $k_f^{(e)}$ and $k_{A \rightarrow B}^{\text{net}}$, we can test whether the system is in a steady-state irreversible regime or not. Our calculations yield nearly equivalent values: $k_f^{(e)} = 4.544 \times 10^{-6}\text{ s}^{-1}$, and $k_{A \rightarrow B}^{\text{net}} = 4.537 \times 10^{-6}\text{ s}^{-1}$, which confirms that the first steady state corresponds to the irreversible isomerization. The population distribution function for isomer A during this period is typical of population functions for irreversible reactions with depleted levels above threshold (Figure 5a) and does not change in shape.

Note that the irreversible regime described above is a consequence of initial distribution between the isomers, which is essentially nonequilibrium: isomer B is zero populated and remains very low populated (less than 1%) during this period, while the equilibrium population of B should be $\sim 50\%$ ($K_c^{\text{eq}} \approx 1^{15}$).

There is another regime of the reaction at $t > 10^4\text{ s}$, which is characterized by a gradual increase of k_f up to its equilibrium value (Figure 4). With increasing time, the population of B below threshold gradually grows (Figure 5b) and activation from those levels becomes significant. This reverse flux from low levels of B (i.e. $B \rightarrow B^*$) makes the distribution function of A

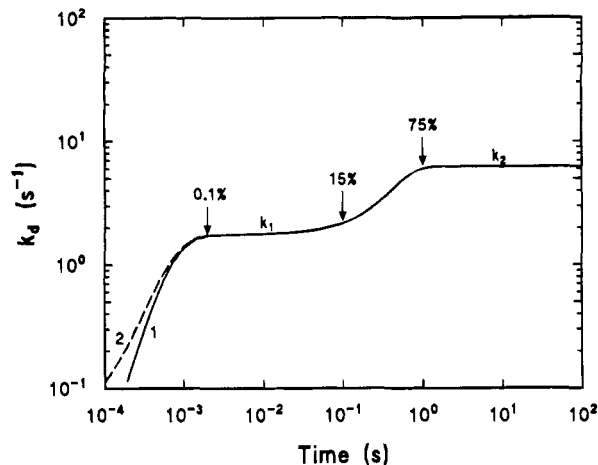


Figure 6. Multiple steady-state behavior of the rate coefficient for the formation of butadiene. The percentage of decomposition of *cis*-2-butene is indicated. $T = 1200$ K. This behavior is independent of the initial population of the *cis* isomer: $T_0 = 300$ (1) and 600 (2) K.

closer to an equilibrium population (curve 4 in Figure 5), and finally, achieve equilibrium at the second plateau at $t > 10^6$ s in Figure 4. The net flux of reaction $k_{A \rightarrow B}^{\text{net}}$ and $k_f^{(e)}$ are no longer equivalent, because reaction net flux gradually approaches zero during this period, while $k_f^{(e)}$ is constant. Thus, the second regime of isomerization is essentially reversible.

IV. Isomerization and Decomposition

At high temperatures, isomerization of *cis*-2-butene is accompanied by side reactions, the most important of which is decomposition of *cis*-2-butene to butadiene and hydrogen. The barrier height for the decomposition channel is higher than that for the isomerization by ~ 9 kJ/mol (800 cm $^{-1}$),¹⁰ which results in negligible decomposition compared to the isomerization at low temperatures,⁸ but substantial decomposition at high temperatures. In considering the high-temperature isomerization, our focus is not the isomerization, but the effect of isomerization on the product (butadiene) formation. We will compare our computations with the results of very low pressure pyrolysis (VLPP) of *cis*-2-butene.¹⁰

In these computations we used the same input parameters for *cis-trans* isomerization as in the previous section. For the transition state for formation of butadiene we used the vibrational frequencies and other parameters: $E_2 = 22\,700$ cm $^{-1}$, $\beta^{\#} = 1$, $\omega = 10^{4.3}$ s $^{-1}$, as indicated by Alfassi et al.¹⁰ Assuming that parameter α increases with temperature and corresponds mainly to wall collisions¹⁰ we put $\alpha = 2000$ cm $^{-1}$.

Even though the frequency ω in the VLPP experiment¹⁰ corresponds mainly to wall collisions, we can find the effective pressure which produces the same collision frequency. Thus from eq 21 we estimate $p_{\text{eff}} = 4 \times 10^{-4}$ kPa, which is close to the lowest pressure in the Rabinovitch experiment.⁸

The rate coefficient for butadiene formation for two different initial populations of A is shown in Figure 6 as a function of time along with the percentage decomposition of *cis*-2-butene. The most interesting feature is the multiple steady-state behavior of the rate coefficient (Figure 6). 15% of the butadiene forms at nearly constant rate coefficient k_1 during the first 0.1 s (the first steady state), while 25% of the product forms at $t > 1$ s at constant rate k_2 corresponding to the true steady state. However, 50% of butadiene formation occurs during a transition period between 0.1 and 1 s, where the rate coefficient gradually changes from k_1 to k_2 . The origin of such behavior can be explained in the same way as the case of equilibrating isomerization: the

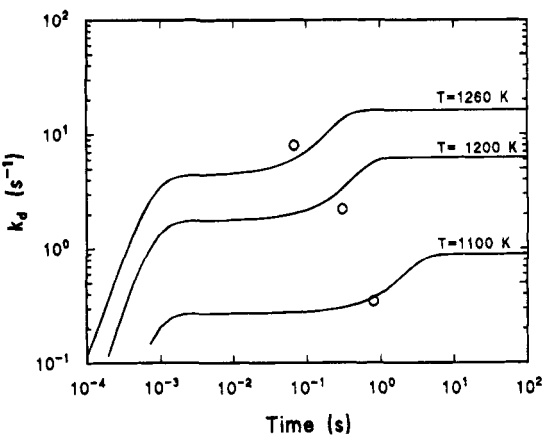


Figure 7. Comparison of the master equation calculations with the VLPP experiment¹⁰ (circles). The experimental conditions correspond to the first steady state.

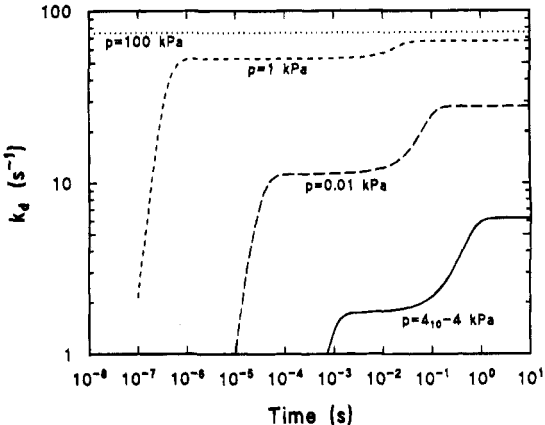


Figure 8. Decomposition rate coefficient versus time at different pressures and $T = 1200$ K.

first plateau corresponds to irreversible isomerization (and decomposition), and the transient period between plateaus corresponds to the late stage of equilibration between A and B, where activation from low B levels is significant, while the second plateau corresponds to the decomposition when equilibration between isomers has already been achieved. We also note that the time evolution of the rate coefficient does not depend on initial population except for the very short induction time ($t < 10^{-3}$ s), where less than 0.1% of the product forms.

Results of our calculations for the rate coefficients at different temperatures are shown in Figure 7 together with the experimental points obtained in VLPP experiment.¹⁰ The positions of the experimental points on a time axis were determined by mapping against the percentage of butadiene formation in VLPP measurements. According to our calculations the experimental points lie at the end of the first steady-state period at each temperature and show good agreement with our k_i values (Figure 7). Thus, we can conclude that the experimental conditions¹⁰ correspond to the first steady state or, in other words, to irreversible isomerization.

It should be noted that this multiple steady-state effect can be observed only at low pressures and at high temperatures, because, at high pressures, population distribution functions are at equilibrium due to rapid collisional energy transfer and hence a constant rate coefficient (Figure 8). At low temperatures, as we have shown, the equilibrating period is sufficiently long so as to be inaccessible in a practical sense. Only the early stages of equilibrating isomerization would be observed, which is essentially irreversible and thus the rate coefficient equals

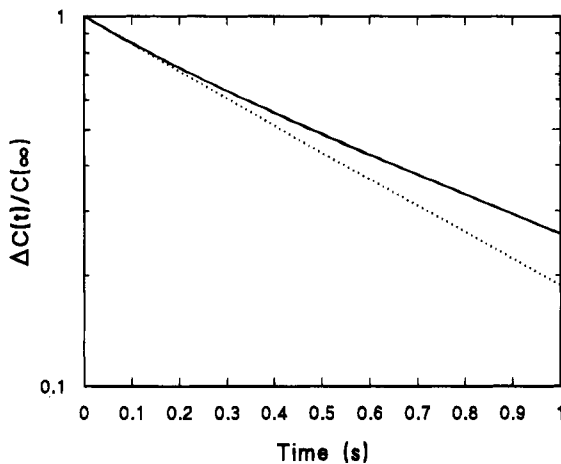


Figure 9. Concentration of the product versus time (solid line). The initial slope is shown as a dotted line. A change in slope is seen at $t = 0.1$ s.

$k_f^{(e)}$ which can be calculated through the equilibrium constant K_c^{eq} and the steady-state relaxation rate coefficient k_{rel} .

As we have mentioned, rate coefficient k_d can be obtained directly from the measurements. In fact, the directly measured quantities are concentrations of A, B, and C, from which k_d is obtained. It is of interest to see how the multiple steady-state behavior of k_d reflects on the time dependencies of concentrations. Indeed, in a pure decomposition system we would expect a straight line if we plot $\Delta C(t) = C(\infty) - C(t)$ on a logarithmic scale versus time. For the system with isomerization, our analysis predicts a change in slope due to the transition from k_1 to k_2 . Figure 9 shows the time evolution of the product concentration from which the deviation from the straight line corresponding to the initial slope is easily seen. However, the change in slope is in contrast to what we could expect from values for k_1 and k_2 (Figure 6). The point is that the slope in Figure 9 is not exactly k_d , but $k_d/(1 + K_c)$ as can be obtained from summation of eqs 1 over i and l and adding the second equation to the first. Indeed, after the summation we have

$$\frac{d(A+B)}{dt} = -k_d A \quad (26)$$

We note that $A + B = C(\infty) - C = \Delta C$ and $A = (A + B)/(1 + K_c)$ from which we obtain

$$\frac{d\Delta C}{dt} = -\frac{k_d}{1 + K_c} \Delta C \quad (27)$$

At the initial time, $K_c \ll 1$ and thus the initial slope gives k_1 . At the late stages of equilibration, K_c becomes closer to its equilibrium value thus lowering the slope. The resulting slope is defined by the ratio of k_d which increases in time (Figure 6) and $1 + K_c$ which increases too (Figure 4). Therefore, the final slope (steady-state slope) is always less than k_2 and might be less than k_1 , if K_c^{eq} is large enough.

V. Conclusions

We have presented the time-dependent master equation analysis for a system with decomposition and isomerization. In a pure isomerization system, there are two regimes during the steady-state equilibration: irreversible isomerization with the time-independent forward rate coefficient and essentially revers-

ible isomerization at late stages of equilibration with both time-dependent forward and reverse rate coefficients. A system with isomerization and decomposition exhibits a multiple steady-state behavior: the first steady state corresponds to the irreversible isomerization at early stages of equilibration between the isomers, while the second steady state establishes after the equilibrium has been achieved. The effect can be observed at low pressures and high temperatures. It can be seen as a change in the slope in the plot of logarithm of the product concentration versus time.

These results may have extremely serious implications on the simulation of the behavior of reacting systems. For such applications, the essential input data are sets of rate constants as a function of temperature and pressure for each single-step reaction. The present results show that even for the simplest isomerization-decomposition system, below a certain pressure, it is not possible to describe the reaction at any temperature and pressure in terms of a single rate constant. We have at the present time no methodology for the treatment of such situations. In addition, the phenomena can be a potential source of error in the interpretation of kinetic results. A measured rate constant, as in Figure 7, may not be applicable under other conditions.

In many ways the phenomena can be considered an extension of the well-known initial incubation time prior to the achievement of a steady-state distribution, where it is not possible to specify a rate constant. This can be seen in many of the accompanying figures. However, unlike the isomerization situation, this is a vibrational relaxation problem and since the time scales are short it can be usually ignored. Actually, in the present case it can be seen that except at the lowest pressures the effect is small and therefore the selection of an average rate constant would not lead to serious errors. We are now investigating the more general situation, including chemically activated systems, so as to more properly assess the importance of the phenomena.

Acknowledgment. The contributions of W.T. to this work was supported by the Department of Energy, Division of Basic Energy Sciences.

References and Notes

- (1) Robinson, P. J.; Holbrook, K. A. *Unimolecular Reactions*; Wiley-Interscience: London, 1972.
- (2) Forst, W. *Theory of Unimolecular Reactions*; Academic: New York, 1973.
- (3) Gilbert, R. G.; Smith, S. C. *Theory of Unimolecular and Recombination Reactions*; Blackwell: Oxford, 1990.
- (4) Quack, M. *Ber. Bunsenges. Phys. Chem.* **1984**, *88*, 94.
- (5) Green, N. J. B.; Marchant, P. J.; Perona, M. J.; Pilling, M. J.; Robertson, S. H. *J. Chem. Phys.* **1992**, *96*, 5896.
- (6) Aguda, B. D.; Pritchard, H. O. *J. Chem. Phys.* **1992**, *96*, 5908.
- (7) Kistiakowsky, G. B.; Smith, W. R. *J. Am. Chem. Soc.* **1936**, *58*, 766.
- (8) Rabinovitch, B. S.; Michel, K. W. *J. Am. Chem. Soc.* **1959**, *81*, 5065.
- (9) Lifshitz, A.; Bauer, S. H.; Resler, Jr., E. L. *J. Chem. Phys.* **1963**, *38*, 2056.
- (10) Alfassi, Z. B.; Golden, D. M.; Benson, S. W. *Int. J. Chem. Kinet.* **1973**, *5*, 991.
- (11) Beyer, T.; Swinehart, D. F. *Comm. Assoc. Comput. Machines* **1973**, *16*, 379.
- (12) Wilkinson, J. H.; Reinsch, C. *Linear Algebra*; Springer: New York, 1971.
- (13) Richards, C. M.; Nielsen, J. R. *J. Opt. Soc. Am.* **1950**, *40*, 442.
- (14) Lin, M. C.; Laidler, K. J. *Trans. Faraday Soc.* **1968**, *64*, 94.
- (15) Benson, S. W.; O'Neal, H. E. *Kinetic Data on Gas Phase Unimolecular Reactions*; NSRDS-NBS 21; U.S. Govt. Printing Office: Washington, DC, 1970.